Surface chemistry controls anomalous ferroelectric behavior in lithium niobate

Sabine M. Neumayer[1,2*], Anton V. Ievlev[2], Liam Collins[2], Rama Vasudevan[2], Mohammad A. Baghban[3], Olga Ovchinnikova[2], Stephen Jesse[2], Katia Gallo[3], Brian J. Rodriguez[1], and Sergei V. Kalinin[2*]

[1]School of Physics, University College Dublin, Dublin, Ireland

[2]Center for Nanophase Materials Science, Oak Ridge National Laboratory, Oak Ridge, TN, USA

[3]Department of Applied Physics, KTH Royal Institute of Technology, Stockholm, Sweden

*Corresponding authors: neumayersm@ornl.gov, sergei2@ornl.gov

Abstract

Polarization switching in ferroelectric materials underpins a multitude of applications ranging from non-volatile memories to data storage to ferroelectric lithography. While traditionally considered to be a functionality of the material only, basic theoretical considerations suggest that switching is expected to be intrinsically linked to changes in the electrochemical state of the surface. Hence, the properties and dynamics of the screening charges can affect or control the switching dynamics. Despite being recognized for over 50 years, analysis of these phenomena remained largely speculative. Here we explore polarization switching on the prototypical $LiNbO_3$ surface using the combination of contact mode Kelvin probe force microscopy and chemical imaging by time-of-flight mass-spectrometry and demonstrate the pronounced chemical differences between the domains. These studies provide a consistent explanation to the anomalous polarization and surface charge behavior observed in $LiNbO_3$ and point to new opportunities in chemical control of polarization dynamics in thin films and crystals via control of surface chemistry, complementing traditional routes via bulk doping and substrate induced strain and tilt systems.

Keywords

Ferroelectrics, surface chemistry, lithium niobate, switching dynamics, scanning probe microscopy, time-of-flight secondary ion mass spectrometry

Introduction

Ferroelectric materials are essential for multiple functional applications including information storage, energy harvesting, electro-optic devices, and electronic circuits.[1–6] The intrinsic polarization in these materials enables applications in non-linear optics, such as waveguides in which quasi phase matching is achieved through periodic domain patterns. Moreover, polarization dependent charge accumulation and band bending at ferroelectric interfaces have led to the development of ferroelectric field effect transistors for non-volatile random access memory. This technology is used in smart cards and based on a binary system where "0" and "1" are encoded in upwards or downward polarization of the ferroelectric gate material.

In a simple physical description, the ferroelectric switching that lies at the heart of these applications is induced by electric fields that control the orientation of polarization depending on the polarity and amplitude of the applied voltage. The polarization aligns dependent on the applied electric field. For example, if a positive voltage is applied to a surface of positive (upwards) polarization, a domain with negative (downwards) polarization forms whereas a negative voltage induces polarization switching from negative to positive orientation. However, even cursory analysis of the thermodynamics of ferroelectric switching suggests a much more complex mechanism.[7–9] Since the polarization is unstable in the absence of screening charges at ferroelectric interfaces, polarization switching necessitates a redistribution of screening charges. On metal electrodes, charges are readily available. Yet, at interfaces with conductors of finite density of states or low mobilities, thermodynamics or kinetics of screening effects can sensitively affect or control switching dynamics. Recently, these phenomena were shown to lead to

ferroionic states,[10] however, these effects can be much more extensive. Therefore, feasibility and performance of applications based on ferroelectric switching are inseparably tied to polarization screening dynamics at ferroelectric surfaces and depend on available internal and external screening charges, electrochemical interactions and ferro-ionic states.[10–13]

As a model material system to study interactions between screening charges and polarization dynamics we have chosen $LiNbO_3$. We used congruently grown $LiNbO_3$ because of its maturity, reproducibility of domain patterning results and well-established electric, piezoelectric and ferroelectric properties.[14–16] The substrates consisted of congruently grown optical grade c-cut LN (conductivity ~3×10^{-6} $m\Omega^{-1}m^{-1}$, dielectric constant ε_{33} =28), used for their piezoelectric and ferroelectric features along the z-axis (piezoelectric strain constant d_{33}=19.22 $\times10^{-11}$ C/N, coercive field E_C = 21kV/mm and spontaneous polarization P_S=75 $\mu C/cm^2$), where domain arrays are routinely and reliably engineered by bulk room-temperature electric field poling techniques.[17]

Apart from being widely used for quasi-phase matching in optics, which necessitates fine domain patterns,[18,19] this material family also shows considerable interesting anomalies in ferroelectric behavior, suggesting strong remanent effects of screening charges. These anomalies comprise a propensity for formation of bubble domains via backswitching,[20–22] unusually large domain wall widths,[23,24] anomalous long surface potential retention in vacuum[25] and fractal domain formation during switching.[19] Moreover, $LiNbO_3$ has shown domain interactions leading to periodic, quasiperiodic to chaotic polarization patterns dependent on screening at the $LiNbO_3$ –water layer interface as well as abnormal switching such as domain instabilities and switching after the application of bias pulses, sparking envisioned technologies beyond conventional applications.[9,12,26] Intriguingly, the morphology of ferroelectric domains arising from anomalous switching in $LiNbO_3$ enables high density encoding of information as specific domain

patterns.[9,26] These patterns of ferroelectric domains are created by particular sequences of bipolar triangular voltage pulses representing a series of binary bits.

Here, we elucidate local ferroelectric behavior across a +z oriented $LiNbO_3$ substrate, (*i.e.,* the polarization vector points upwards) and macroscopically switched -z domains using piezoresponse force microscopy (PFM). The sample was annealed after poling. Nominally, polarization switching on +z and -z surfaces should be equivalent, however, in practice, asymmetries can arise from memory effects.[23,27] In poled domains, the existence of electric fields originating from frustrated defects facilitates backswitching to the original polarization state. However, symmetry is widely restored by annealing.

Therefore, we study polarization switching between +z and -z states on initially +z and -z oriented surfaces, leading to 4 states in total. These states are expected to be pairwise equivalent in the absence of anomalous effects.

PFM is commonly used to study micro- and nanoscale electromechanical properties by monitoring the piezoelectric behavior of a sample in response to an ac excitation voltage supplied to a conductive atomic force microscopy (AFM) tip in contact with the sample. For ferroelectrics materials, PFM can be combined with related switching spectroscopy techniques such that an additional dc voltage (above the coercive field of the sample) is applied to induce polarization switching in the material. However, it is largely accepted that the PFM signals can not only originate from electromechanical strain but also from hysteretic surface charging and corresponding electrostatic interactions between tip and sample.[28,29] Indeed, in certain cases, characteristic hysteresis loops, reminiscent of polarization-dependent piezoelectric strain in standard ferroelectrics, can be observed on non-ferroelectric materials or on ferroelectrics below coercive fields.[30–32] These effects are often due to a combination of surface charging, additive surface electrochemistry and piezoelectric effects. To distinguish these contributions as well as to gain insight into polarization dynamics, contact Kelvin probe force microscopy (cKPFM)[28] was developed, and used here to investigate ferroelectric properties and polarization switching in $LiNbO_3$. By combining it with chemical

imaging using time-of-flight mass-spectrometry (ToF-SIMS), we demonstrate a complex interplay between polarization switching dynamics and surface chemistry as well as pronounced chemical differences between domains.

Results and discussion

In cKPFM, dc write pulses of successively increasing and decreasing amplitude of both polarities are applied to induce ferroelectric switching. In standard switching spectroscopy PFM,[33,34] no dc voltage is applied between those pulses during the read steps. cKPFM, however, utilizes a low dc read voltage during the read step that is sequentially increased with each write cycle to control electrostatic forces, which provides additional information on the number of polarization states, the junction contact potential difference (jCPD) and dielectric properties. The applied waveform envelope consisting of write cycles between ±90 V and read voltages between -9 V and +9 V is depicted in the supporting information (Figure S1). The resulting 2-dimensional cKPFM diagrams, showing the measured response during read steps (y-axis) as a function of the applied read voltage (x-axis) after each write pulse (color coded), provide information on ferroelectric switching. The y-intercept at 0 V read voltage corresponds to the classic PFM signal whereas the x-intercept provides a measure of the jCPD and can be related to surface charging effects. cKPFM therefore provides a more complete picture than standard switching spectroscopy PFM.

Figure 1 shows standard band excitation PFM[35,36] images acquiredbefore and after cKPFM spectroscopy to study polarization switching by cKPFM. While topography appears uniform across the whole scan, band excitation PFM images show a decrease in amplitude for the macroscopically poled hexagonal -z domain compared to the +z oriented substrate, indicating a weaker piezoelectric activity (Figure 1(a)). The difference in PFM amplitude is accompanied by a weak phase contrast that is much smaller than the expected difference of π that is usually associated with a change in polarization orientation.

However, this PFM artefact is common with $LiNbO_3$ and has been related to electrostatic interactions.[37] The resonance frequency shifts only a few kHz within the scan but does not show a strong correlation with the domain pattern. Since the resonance frequency changes with elastic modulus we can conclude that there are small changes in tip state mainly along the slow scan axis but that the +z substrate and -z domain do not exhibit different elastic properties.

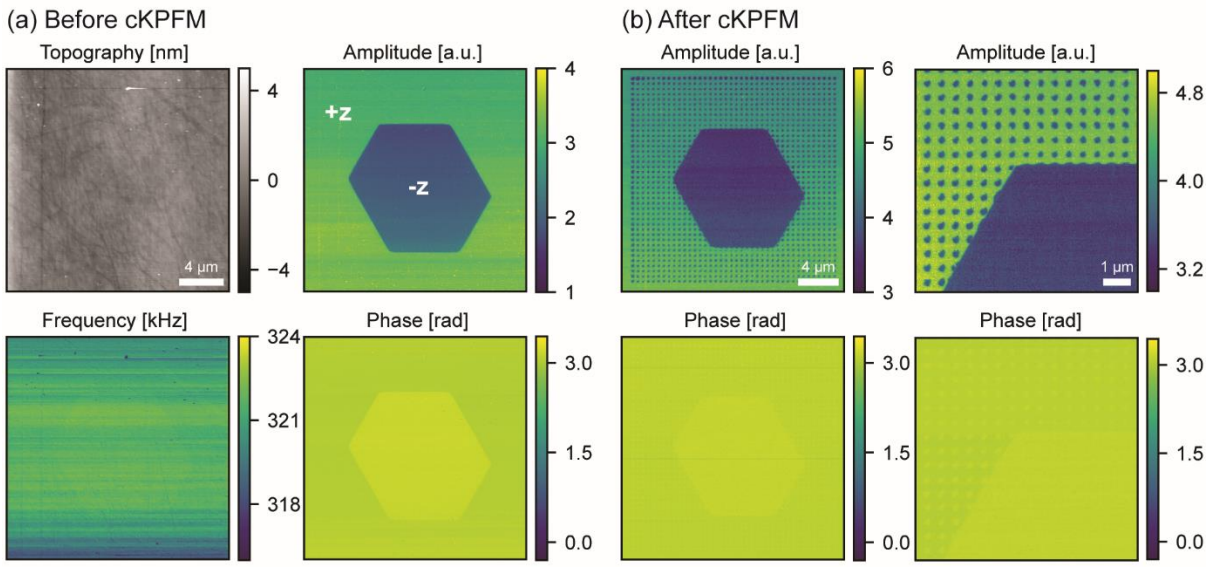

Figure 1 (a) Topography image and maps of band excitation PFM amplitude, phase and resonance frequency before cKPFM spectroscopy (b) band excitation PFM amplitude and phase images recorded after cKPFM spectroscopy at different scan sizes.

In the aforementioned 2-dimensional diagrams obtained from cKPFM spectroscopy, the formation of two distinct bands is observed within the +z substrate (Figure 2(a)) whereas the macroscopically poled -z domain shows only one band (Figure 2(b)). Moreover, the orientation of the loops acquired during the read steps is opposite for +z substrate and -z domains (Figure 2(c,d), however, the phase is nearly constant for all pixels and does not exhibit the expected change of π for the +z substrate. As reported in previous

papers,[10,28] these cKPFM characteristics provide evidence for ferroelectric switching on the +z substrate whereas the observed behavior on the -z domain would suggest no ferroelectric switching and only electrostatic interactions within the applied dc voltage waveform between ±90 V. The sample used in this study was annealed after macroscopic poling, leading to reorientation of defect dipoles[23] and symmetry between domains during silver photodeposition experiments and Raman measurements,[38] thus the observed strong asymmetries in switching behavior are unexpected. A strong imprint is noticeable in loops shown in Figure 2(c) where switching to positive domains occurs at lower voltages than for negative domains for all read cycles. Moreover, hysteresis loops shift along the x-axis to more positive write voltage values with increasingly positive read voltages. However, as expected, especially at higher positive and negative read steps, the measured response is heavily affected by electrostatic tip - sample interactions.

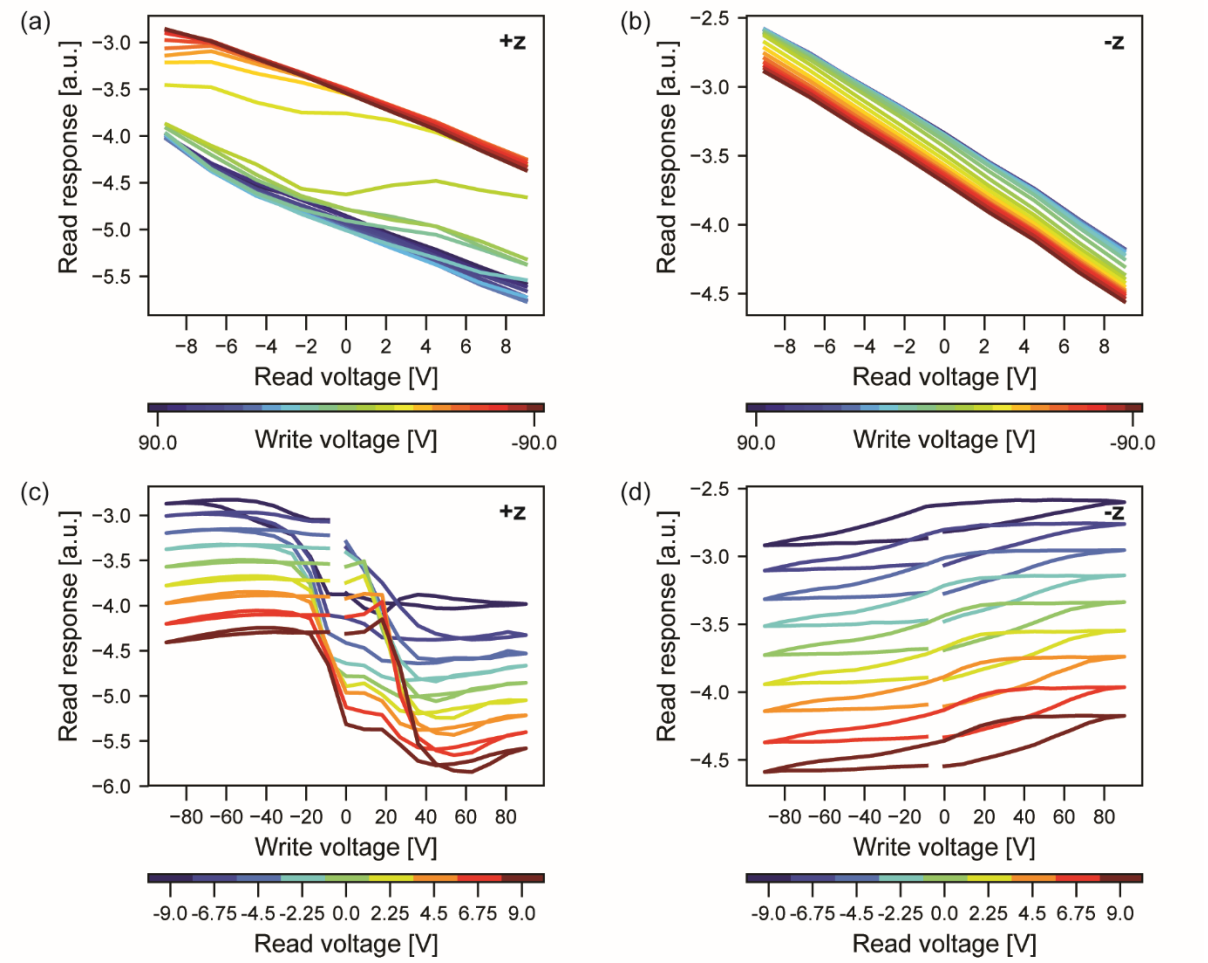

Figure 2 (a,b) cKPFM response measured during read steps between write pulses from +90 V to -90 V (color coded) depicted as function of read voltage and (c,d) cKPFM response for each read step (color coded) as a function of write voltage. Acquired from (a,c) the +z substrate and (b,d) the macroscopically -z domain.

After cKPFM spectroscopy measurements across the depicted area, domain patterns due to polarization switching are apparent within the +z substrate (Figure 1(b)). As band excitation PFM images at different scan sizes show, these local domains exhibit the same amplitude and phase contrast as the macroscopically poled -z domain. Moreover, the domain pattern is stable within several band excitation PFM scans and even hours after cKPFM spectroscopy. However, since the write cycle ends with negative

voltages, the observed pattern of negative domains within the +z substrate is unexpected. The loops depicting cKPFM response during each read voltage step (color coded) show full switching on the +z substrate even for the last cycle, suggesting that the observed domain contrast originates from backswitching to an apparently more stable -z domain after cKPFM. It is known that resulting domain patterns and ferroelectric behavior in $LiNbO_3$ can also strongly depend on available external screening charge at the surface, which is usually provided by the water layer that covers all surfaces in non-dry conditions.[11,12,39]

To study the impact of external screening charge on the surface, the experiment was repeated upon using a deionizing fan, which neutralizes external screening charges. However, the main peculiarities persist (see Figure S2 in supporting information): (i) Polarization switching was only observed for the +z substrate although under deionization a phase contrast of π was measured between domains in both cKPFM spectroscopy and band excitation PFM scans and (ii) locally switched negative domains appeared within the +z substrate.

The 2-dimensional graphs in Figure 2 show cKPFM data averaged over pixels within the +z substrate and the -z domain. In a next step, we extend the cKPFM technique to a spatially resolved imaging technique for the first time. In this way, characteristic spatial variation was extracted by fitting the read response vs. read voltage to a linear function for each point of the spectroscopic grid. Under this scheme, the x-intercept that corresponds to the jCPD, the slope which is related to dielectric properties and the y-intercept indicating the response in absence of an additional dc voltage, can be extracted locally for each pixel.[29] In Figure 3, we show maps composited of these local fitting parameters extracted for the highest and lowest write voltages of +90 V and -90 V, respectively. A pronounced contrast is visible at +90 V where pixels within the macroscopically poled -z domain exhibit lower negative values for the jCPD, steeper negative slopes and lower negative y-intercept values than the surrounding substrate (Figure 3(a)).

At -90 V, the overall trend persists but the contrast is lowered (Figure 3(b)). The similarities at -90 V could arise from similar electrostatics due to injection of electronic charges at high negative write voltages. Surface chemistry induced by positive voltage pulses seems to be specific to domain polarity, whereas negative voltages are much less sensitive to polarization orientation.

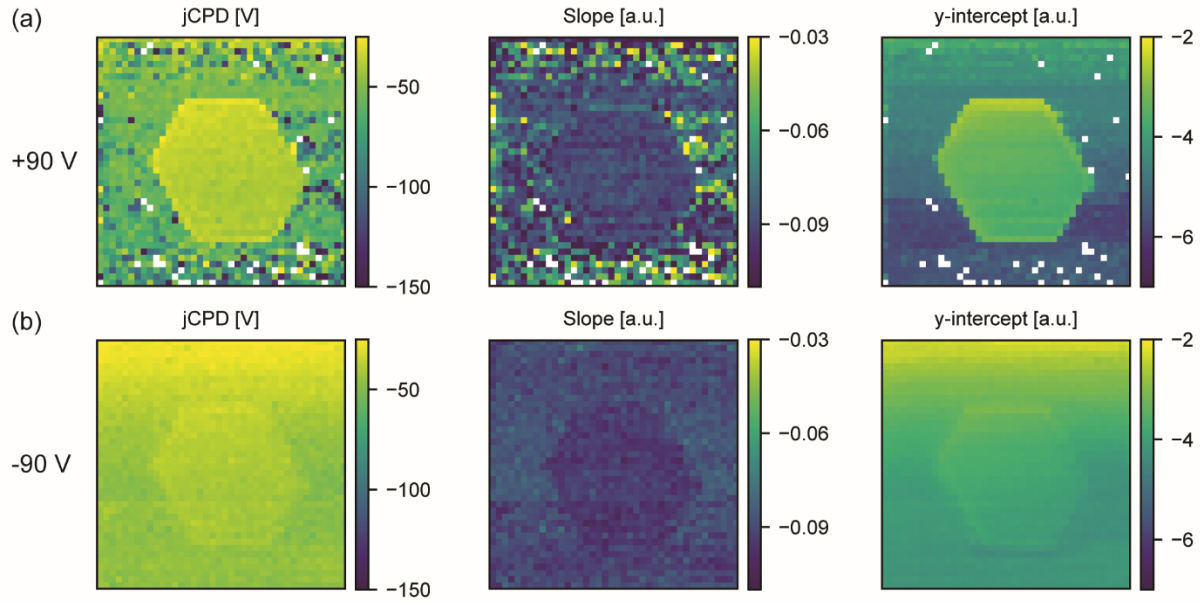

Figure 3 Maps of jCPD, slope and y-intercept obtained from fitting the cKPFM response vs. read voltage (as shown in Figure 2(a,b)) to a linear function for lines obtained at (a) +90 V and (b) -90 V. White pixels correspond to bad fits, image size 20×20 μm^2.

Therefore, the anomalies observed with cKPFM and PFM comprise (i) an asymmetry in ferroelectric behavior between the +z substrate and -z domain where ferroelectric switching only occurs for +z within dc write pulses between ±90 V, (ii) formation of locally switched -z domains within the +z substrate although the last write polarity is negative, (iii) the surface chemistry appears to be sensitive to polarization only for positive dc write pulses. While external screening charges can be ruled out as cause

of these peculiarities, they can be explained by considering the presence of chemical changes on the surface or in the bulk.

To gain insight into the intrinsic surface chemistry, we utilized ToF-SIMS in the positive ion detection mode. In these measurements, surface layers of the $LiNbO_3$ sample were bombarded by a focused Bi_3^+ beam and the released secondary positive ions were detected and identified using time-of-flight detector. For chemical investigations in the bulk we introduced an O_2^- sputter gun into the measurement scheme. Depth profiling measurements were carried out in non-interlaced mode, where every SIMS scan with Bi_3^+ ions was followed by sputtering with O_2^- ion gun.

Chemical imaging revealed that the surface chemistry differs greatly for the +z substrate and -z domain (Figure 4). From the full mass spectra collected by ToF-SIMS we selected peaks corresponding to the base $LiNbO_3$ elements $^6Li^+$, Nb^+, NbO_2^+ and the peak of $C_2H_5^+$, which corresponds to surface contamination and showed spatial correlation with polarization. The $^6Li^+$ isotope was used due to the saturation of the base Li^+ signal.

Analysis of the surface ToF-SIMS data (Figure 4a) showed an increase of the $^6Li^+$, NbO_2^+ and C^2H^{5+} concentration inside -z domains with respect to +z substrate. Depth profiling revealed that in the case of $^6Li^+$ and NbO_2^+ these changes propagate deeper than 120 nm and in the case of contaminant $C_2H_5^+$ are localized on the surface. At the same time, Nb^+ did not show any spatial distribution associated with polarization. ToF-SIMS results can be affected by the presence of internal electric fields, as imaging is based on the interaction of the sample with the focused ion beam and analysis of released secondary ions. In this case, sputter yields would be altered too, leading to different sputter rates within different domains. However,AFM imaging of the sputtered regions did not show any topographic differences between domains, indicating that the sputter rate was not polarization dependent.

The positive ion detection mode used in this study, does not allow to directly measure the concentration of O^- ions. However, clusters containing oxygen can give information on the O^- concentration. Since there is no spatial variation in the Nb^+ map, but contrast in NbO_2^+, we can conclude that the -z domains contain more oxygen. Similarly, $^6Li^+$ was found to exhibit a higher concentration inside the -z domains.

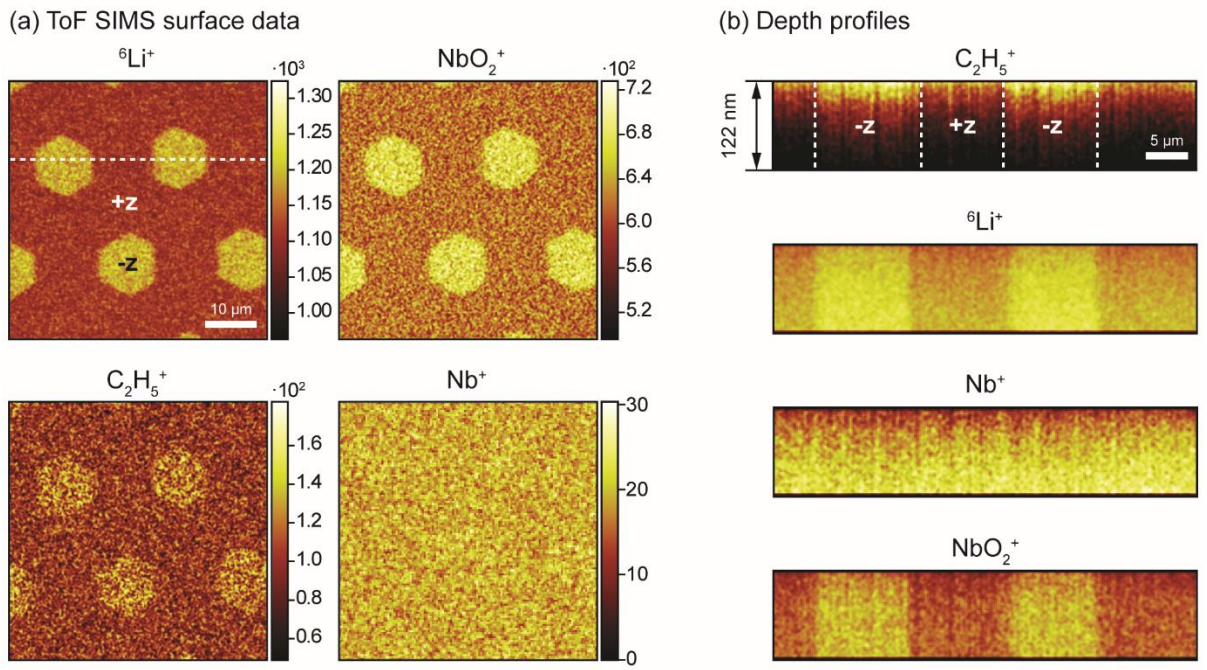

Figure 4 Tof SIMS analysis (a) surface data averaged over the whole sputter time (b) depth profiles of section indicated by horizontal dashed line in (a) showing concentration over sputtering depth, vertical dashed lines indicate boundaries between +z and -z domains.

The evidently different surface chemistry of the +z substrate and the macroscopically poled -z domain are likely the explanation for the observed switching asymmetries and local backswitching within the +z substrate. The higher concentration of positive ions within the -z domain surface presumably originates from field-induced ion migration during the annealing process that increases ion mobility and

provides effective internal screening, stabilizing the negative polarization. These positive ions at the -z surface are expected to prevent switching to positive domains within the applied voltage range used for cKPFM. The +z substrate, however, is presumably not well screened as mainly positive ions such as Li^+ and H^+ are mobile during the annealing process. The coercive field of undoped congruent lithium niobate is ~20 kV/mm,[23] however, in PFM experiments, ferroelectric switching can occur at much lower voltages due to the field localization at the tip apex and nucleation at sample defects.[40,41] The lower concentration of $^6Li^+$ points to a higher concentration of Li vacancies within the +z substrate, which might facilitate domain nucleation and further contribute to the observed switching asymmetries. The backswitching to local negative domains within the +z substrate could be initiated by the positive polarity of the last read voltage pulse and further facilitated by highly mobile electronic charge that is available from electron injection during negative write pulses. Furthermore, the high negative write pulses could cause field-induced transport of positive ionic charge towards the surface, as previously observed in bismuth ferrite.[42] Moreover, contamination with positively charged hydrocarbons is also evident within the +z substrate and might provide additional screening charge to stabilize the small negative domains that form after the tip moves to the next pixel and the metal coating cannot further provide screening.

To summarize, we have explored the interplay between polarization switching dynamics and surface chemistry of annealed macroscopically periodically poled $LiNbO_3$. The surface composition was found to be strongly dependent on polarization, which was attributed to the increased ion mobility at high temperatures that leads to ion migration dependent on internal electric fields. According to screening considerations and previous reports, annealed $LiNbO_3$ is expected to show a higher O^- concentration at +z surfaces than for -z. However, the higher oxygen content within the -z domain observed in this work can likely be ascribed to electric field-induced oxygen diffusion during the macroscopic poling process similar to changes in surface chemistry observed in bismuth ferrite.[42] This additional negative charge is anticipated to contribute to the attraction of positive charges during and after the annealing step. Tied to the availability

of internal and external screening charge, the higher contents of positive ionic compounds observed in ToF-SIMS for $^{6}Li^{+}$, and $C_2H_5^{+}$ contamination stabilize the polarization of the negative domain, which did not exhibit ferroelectric switching within the applied write voltage pulses between ±90 V.

Within the +z substrate, ferroelectric switching is evident from the formation of two bands in the cKPFM graphs, indicating two polarization states. After cKPFM spectroscopy, locally switched domains of negative polarity are visible in the +z substrate, despite the write cycle ending with negative voltage pulses. The apparent local backswitching, that also occurs upon neutralizing external screening charges, is attributed to a combination of: (i) nucleation initiated by the positive read voltage pulse applied as the last step, (ii) availability of mobile screening charges by electron injection during the negative write pulses, (iii) field-induced migration of positive ions during the application of high negative voltage pulses and (iv) $C_2H_5^{+}$ surface contamination, which is also evident within the +z substrate.

Therefore, sample processing steps such as annealing can be crucial to ferroelectric behavior and to the obtained domain patterns. The impact of surface chemistry on the electromechanical behavior can be utilized by introducing negative domains in a positive substrate before annealing thus locally disabling polarization switching within a certain voltage range. In addition, backswitching phenomena can be utilized to obtain fine domain patterns and provide further insight into the role of internal screening charges on ferroelectric behavior. Moreover, these studies illustrate a strong coupling between surface chemistry and polarization switching, which, while demonstrated here for $LiNbO_3$, is also expected for other ferroelectric materials. We also note that classical ways to control material properties are through doping in bulk crystals or substrate strain[43–46] and octahedra tilt systems[47–49] in films. Here, we show that the long-range nature of ferroelectricity and its sensitivity to screening also enables control via surface chemistry, both by thermodynamics of screening charges that affects polarization stability[10] and by their kinetics, as discovered

here. These insights on coupling between chemistry and polarization open up future opportunities for applications in information storage, in energy harvesting and in elements for electronic devices.

Acknowledgements

Scanning probe microscopy and ToF-SIMS were conducted at the Center for Nanophase Materials Sciences, which is a DOE Office of Science User Facility. The scanning probe microscopy part of this work was supported by the U.S. Department of Energy, Office of Science, Basic Energy Sciences (S.M.N.) and Materials Sciences and Engineering Division (R.K.V., S.V.K., S.M.N.). This work has in part emanated from research supported by a research grant from Science Foundation Ireland (SFI) under the US-Ireland R&D Partnership Programme Grant Number SFI/14/US/I3113 (S.M.N., B.J.R.). Data analysis was partially performed using pycroscopy (https://pycroscopy.github.io/pycroscopy/).

Material and Methods

A congruent $LiNbO_3$ substrate (CasTec Inc., dimensions 16×11 mm^2, thickness: 500 μm) was macroscopically poled by applying a voltage of 11 kV to gel electrodes that covered periodical hexagonal openings in a photoresist mask on the –z side whereas on the +z side whole the whole surface was in contact with the electrode. The sample was subsequently annealed for 12 h at 200°C in an oven (Memmert UP400) with a heating/ cooling rate of 3°C/s.

An Asylum Research MFP-3D atomic force microscopy equipped with a high voltage amplifier and National Instrument data acquisition units interfaced with LabView was used for cKPFM spectroscopy. Band excitation PFM and cKPFM were performed with conductive Budgetsensor Multimode probes (nominal force constant = 3 N/m, nominal resonance frequency = 75 kHz). The deionizing fan used for control measurements was a 963E SCS Benchtop Air Ionizer.

PFM images and cKPFM were acquired in band excitation mode where an ac voltage is applied in a frequency band centered around the contact resonance. The resulting response is fitted to a simple harmonic oscillator model from which amplitude, phase, contact resonance and Q-factor can be extracted. The cKPFM waveform comprises 40 dc voltage write steps between ±90 V and 9 dc voltage read steps from -9 V to +9 V (see Figure SI 1) and was applied in maps of 40x40 pixels over a 20x20 μm^2 area.

ToF-SIMS measurements were performed in positive ion detection mode with a TOF SIMS-5 instrument (ION-TOF GmbH). A Bi_3^+ ion beam with an energy of 30 keV, a current of ~0.5 nA and a spot size of ~100 nm was used as a primary source. An O_2^- ion gun of 1keV energy and a current of ~250 nA was used as a sputter source for depth profiling. AFM calibration after sputtering revealed sputter rate about 0.034 nm/s. Chemical imaging was carried out in non-interlaced mode, where every SIMS scan by primary gun ions was followed by sputtering.

Supporting Information. Figure of DC voltage sequence applied in cKPFM spectroscopy. Results upon using a deionizer: band excitation amplitude and phase images after cKPFM spectroscopy and cKPFM graphs.

References

(1) Scott, J. F.; Paz de Araujo, C. A. Ferroelectric Memories. *Science.* **1989**, *246* (4936), 1400 LP-1405.

(2) Waser, R.; Rüdiger, A. Pushing Towards the Digital Storage Limit. *Nat. Mater.* **2004**, *3*, 81.

(3) Shur, V. Y.; Rumyantsev, E. L.; Nikolaeva, E. V; Shishkin, E. I.; Batchko, R. G.; Miller, G. D.; Fejer, M. M.; Byer, R. L. Regular Ferroelectric Domain Array in Lithium Niobate Crystals for Nonlinear Optic Applications. *Ferroelectrics* **2001**, *236*, 129–144.

(4) Dagdeviren, C.; Yang, B. D.; Su, Y.; Tran, P. L.; Joe, P.; Anderson, E.; Xia, J.; Doraiswamy, V.; Dehdashti, B.; Feng, X.; Lu, B.; Poston, R.; Khalpey, Z.; Ghaffari, R.; Huang, Y.; Slepian, M. J.; Rogers, J. A. Conformal Piezoelectric Energy Harvesting and Storage from Motions of the Heart, Lung, and Diaphragm. *Proc. Natl. Acad. Sci. U. S. A.* **2014**, *111* (5), 1927–1932.

(5) Maksymovych, P.; Seidel, J.; Chu, Y. H.; Wu, P.; Baddorf, A. P.; Chen, L. Q.; Kalinin, S. V.; Ramesh, R. Dynamic Conductivity of Ferroelectric Domain Walls in $BiFeO_3$. *Nano Lett.* **2011**, *11* (5), 1906–1912.

(6) Guo, R.; You, L.; Zhou, Y.; Lim, Z. S.; Zou, X.; Chen, L.; Ramesh, R.; Wang, J. Non-Volatile Memory Based on the Ferroelectric Photovoltaic Effect. *Nat. Commun.* **2013**, *4* (May), 1990.

(7) Wang, R. V.; Fong, D. D.; Jiang, F.; Highland, M. J.; Fuoss, P. H.; Thompson, C.; Kolpak, A. M.; Eastman, J. A.; Streiffer, S. K.; Rappe, A. M.; Stephenson, G. B. Reversible Chemical Switching of a Ferroelectric Film. *Phys. Rev. Lett.* **2009**, *102* (4), 2–5.

(8) Kalinin, S.; Bonnell, D. Local Potential and Polarization Screening on Ferroelectric Surfaces. *Phys. Rev. B* **2001**, *63* (12), 125411.

(9) Ievlev, A. V.; Morozovska, A. N.; Eliseev, E. A.; Shur, V. Y.; Kalinin, S. V. Ionic Field Effect and Memristive Phenomena in Single-Point Ferroelectric Domain Switching. *Nat. Commun.* **2014**, *5*, 1–8.

(10) Yang, S. M.; Morozovska, A. N.; Kumar, R.; Eliseev, E. A.; Cao, Y.; Mazet, L.; Balke, N.; Jesse, S.; Vasudevan, R. K.; Dubourdieu, C.; Kalinin, S. V. Mixed Electrochemical–Ferroelectric States in Nanoscale Ferroelectrics. *Nat. Phys.* **2017**, *13*, 1–8.

(11) Neumayer, S. M.; Strelcov, E.; Manzo, M.; Gallo, K.; Kravchenko, I. I.; Kholkin, A. L.; Kalinin, S. V.; Rodriguez, B. J. Thickness, Humidity, and Polarization Dependent Ferroelectric Switching and Conductivity in Mg Doped Lithium Niobate. *J. Appl. Phys.* **2015**, *118* (24), 244103.

(12) Ievlev, A. V.; Jesse, S.; Morozovska, A. N.; Strelcov, E.; Eliseev, E. A.; Pershin, Y. V.; Kumar, A.; Shur, V. Y.; Kalinin, S. V. Intermittency, Quasiperiodicity and Chaos in Probe-Induced Ferroelectric Domain Switching. *Nat. Phys.* **2014**, *10*, 59–66.

(13) Kalinin, S. V; Morozovska, A. N.; Chen, L. Q.; Rodriguez, B. J. Local Polarization Dynamics in Ferroelectric Materials. *Reports Prog. Phys.* **2010**, *73* (5), 056502.

(14) Weis, R.; Gaylord, T. Lithium Niobate: Summary of Physical Properties and Crystal Structure R. *Appl. Phys. A Mater. Sci. Process.* **1985**, *37* (4), 191–203.

(15) Lines, M. E.; Glass, A. M. *Principles and Applications of Ferroelectrics and Related Materials*; Oxford University Press: Oxford, **2001**.

(16) Kovacs, L.; Polgar, K. Electrical Conductivity of $LiNbO_3$, in EMIS Datareviews Series 28 *Properties of Lithium Niobate*; Wong, K.K. (Ed), IEE INSPEC, London **2002**.

(17) Gallo, K.; Gawith, C. B. E.; Smith, P. G. R. Bidimensional Hexagonal Poling of $LiNbO_3$ for Nonlinear Photonic Crystals and Quasi-Crystals. *Ferroelectrics* **2006**, *340* (1), 69–74.

(18) Manzo, M.; Laurell, F.; Pasiskevicius, V.; Gallo, K. Two-Dimensional Domain Engineering in LiNbO_3 via a Hybrid Patterning Technique. *Opt. Mater. Express* **2011**, *1* (3), 365.

(19) Shur, V. Y.; Akhmatkhanov, A. R.; Baturin, I. S. Micro- and Nano-Domain Engineering in Lithium Niobate. *Appl. Phys. Rev.* **2015**, *2* (4), 040604.

(20) Lilienblum, M.; Soergel, E. Anomalous Domain Inversion in LiNbO3 Single Crystals Investigated by Scanning Probe Microscopy. *J. Appl. Phys.* **2011**, *110* (5).

(21) Kan, Y.; Bo, H.; Lu, X.; Cai, W.; Liu, Y.; Zhu, J. Growth Evolution and Decay Properties of the Abnormally Switched Domains in LiNbO3 Crystals. *Appl. Phys. Lett.* **2008**, *92* (17), 172910.

(22) Shur, V. Y.; Rumyantsev, E. L.; Nikolaeva, E. V.; Shishkin, E. I.; Fursov, D. V.; Batchko, R. G.; Eyres, L. A.; Fejer, M. M.; Byer, R. L. Nanoscale Backswitched Domain Patterning in Lithium Niobate. *Appl. Phys. Lett.* **2000**, *76*, 143.

(23) Gopalan, V.; Dierolf, V.; Scrymgeour, D. A. Defect–Domain Wall Interactions in Trigonal Ferroelectrics. *Annu. Rev. Mater. Res.* **2007**, *37* (1), 449–489.

(24) Choudhury, S.; Li, Y.; Odagawa, N.; Vasudevarao, A.; Tian, L.; Capek, P.; Dierolf, V.; Morozovska, A. N.; Eliseev, E. a.; Kalinin, S.; Cho, Y.; Chen, L. Q.; Gopalan, V. The Influence of 180° Ferroelectric Domain Wall Width on the Threshold Field for Wall Motion. *J. Appl. Phys.* **2008**, *104* (8), 6–8.

(25) Liu, X.; Kitamura, K.; Terabe, K. Surface Potential Imaging of Nanoscale $LiNbO_3$ Domains Investigated by Electrostatic Force Microscopy. *Appl. Phys. Lett.* **2006**, *89* (13), 132905.

(26) Ievlev, A.; Kalinin, S. V. Data Encoding Based on the Shape of the Ferroelectric Domains Produced by the a Scanning Probe Microscopy Tip. *Nanoscale* **2015**, *7*, 11040–11047.

(27) Gopalan, V.; Gupta, M. C. Origin and Characteristics of Internal Fields in $LiNbO_3$ Crystals.

Ferroelectrics **1997**, *198* (1), 49–59.

(28) Balke, N.; Maksymovych, P.; Jesse, S.; Herklotz, A.; Tselev, A.; Eom, C.; Kravchenko, I. I.; Yu, P.; Kalinin, S. V. Differentiating Ferroelectric and Nonferroelectric Electromechanical Effects with Scanning Probe Microscopy. *ACS Nano* **2015**, *9* (6), 6484–6492.

(29) Balke, N.; Maksymovych, P.; Jesse, S.; Kravchenko, I. I.; Li, Q.; Kalinin, S. V. Exploring Local Electrostatic Effects with Scanning Probe Microscopy: Implications for Piezoresponse Force Microscopy and Triboelectricity. *ACS Nano* **2014**, *8* (10), 10229–10236.

(30) Kim, B.; Seol, D.; Lee, S.; Lee, H. N.; Kim, Y. Ferroelectric-like Hysteresis Loop Originated from Non-Ferroelectric Effects. *Appl. Phys. Lett.* **2016**, *109* (10).

(31) Vasudevan, R. K.; Balke, N.; Maksymovych, P.; Jesse, S.; Kalinin, S. V. Ferroelectric or Non-Ferroelectric: Why so Many Materials Exhibit "Ferroelectricity" on the Nanoscale. *Appl. Phys. Rev.* **2017**, *4* (2).

(32) Seol, D.; Kim, B.; Kim, Y. Non-Piezoelectric Effects in Piezoresponse Force Microscopy. *Curr. Appl. Phys.* **2017**, *17* (5), 661–674.

(33) Balke, N.; Bdikin, I.; Kalinin, S. V.; Kholkin, A. L. Electromechanical Imaging and Spectroscopy of Ferroelectric and Piezoelectric Materials: State of the Art and Prospects for the Future. *J. Am. Ceram. Soc.* **2009**, *92* (8), 1629–1647.

(34) Jesse, S.; Baddorf, A. P.; Kalinin, S. V. Switching Spectroscopy Piezoresponse Force Microscopy of Ferroelectric Materials. *Appl. Phys. Lett.* **2006**, *88*, 062908.

(35) Jesse, S.; Vasudevan, R. K.; Collins, L.; Strelcov, E.; Okatan, M. B.; Belianinov, A.; Baddorf, A. P.; Proksch, R.; Kalinin, S. V. Band Excitation in Scanning Probe Microscopy: Recognition and Functional Imaging. *Annu. Rev. Phys. Chem.* **2014**, *65*, 519–536.

(36) Jesse, S.; Kalinin, S. V.; Proksch, R.; Baddorf, A. P.; Rodriguez, B. J. The Band Excitation Method in Scanning Probe Microscopy for Rapid Mapping of Energy Dissipation on the Nanoscale. *Nanotechnology* **2007**, *18*, 435503.

(37) Kim, S.; Seol, D.; Lu, X.; Alexe, M.; Kim, Y. Electrostatic-Free Piezoresponse Force Microscopy. *Sci. Rep.* **2017**, *7* (December 2016), 41657.

(38) Carville, N. C.; Neumayer, S. M.; Manzo, M.; Baghban, M.-A.; Ivanov, I. N.; Gallo, K.; Rodriguez, B. J. Influence of Annealing on the Photodeposition of Silver on Periodically Poled Lithium Niobate. *J. Appl. Phys.* **2016**, *054102*, 1–7.

(39) Ievlev, a. V.; Morozovska, a. N.; Shur, V. Y.; Kalinin, S. V. Humidity Effects on Tip-Induced Polarization Switching in Lithium Niobate. *Appl. Phys. Lett.* **2014**, *104* (9).

(40) Kalinin, S. V.; Gruverman, A.; Rodriguez, B. J.; Shin, J.; Baddorf, a. P.; Karapetian, E.; Kachanov, M. Nanoelectromechanics of Polarization Switching in Piezoresponse Force Microscopy. *J. Appl. Phys.* **2005**, *97*, 075305.

(41) Jesse, S.; Rodriguez, B. J.; Choudhury, S.; Baddorf, A. P.; Vrejoiu, I.; Hesse, D.; Alexe, M.; Eliseev, E. a; Morozovska, A. N.; Zhang, J.; Chen, L.-Q.; Kalinin, S. V. Direct Imaging of the Spatial and Energy Distribution of Nucleation Centres in Ferroelectric Materials. *Nat. Mater.* **2008**, *7*, 209–215.

(42) Ievlev, A. V.; Maksymovych, P.; Trassin, M.; Seidel, J.; Ramesh, R.; Kalinin, S. V.; Ovchinnikova, O. S. Chemical State Evolution in Ferroelectric Films during Tip-Induced Polarization and Electroresistive Switching. *ACS Appl. Mater. Interfaces* **2016**, *8* (43), 29588–29593.

(43) Chen, Y. B.; Sun, H. P.; Katz, M. B.; Pan, X. Q.; Choi, K. J.; Jang, H. W.; Eom, C. B. Interface Structure and Strain Relaxation in $BaTiO_3$ Thin Films Grown on $GdScO_3$ and $DyScO_3$ Substrates

with Buried Coherent $SrRuO_3$ Layer. *Appl. Phys. Lett.* **2007**, *91* (25), 252906.

(44) Sun, H. P.; Tian, W.; Pan, X. Q.; Haeni, J. H.; Schlom, D. G. Evolution of Dislocation Arrays in Epitaxial $BaTiO_3$ Thin Films Grown on (100) $SrTiO_3$. *Appl. Phys. Lett.* **2004**, *84* (17), 3298–3300.

(45) Schlom, D. G.; Chen, L.-Q.; Eom, C.-B.; Rabe, K. M.; Streiffer, S. K.; Triscone, J.-M. Strain Tuning of Ferroelectric Thin Films. *Annu. Rev. Mater. Res.* **2007**, *37* (1), 589–626.

(46) Johnson-Wilke, R. L.; Wilke, R. H. T.; Yeager, C. B.; Tinberg, D. S.; Reaney, I. M.; Levin, I.; Fong, D. D.; Trolier-McKinstry, S. Phase Transitions and Octahedral Rotations in Epitaxial Ag(TaxNb1−x)O3 Thin Films under Tensile Strain. *J. Appl. Phys.* **2015**, *117* (8), 85309.

(47) Borisevich, A. Y.; Chang, H. J.; Huijben, M.; Oxley, M. P.; Okamoto, S.; Niranjan, M. K.; Burton, J. D.; Tsymbal, E. Y.; Chu, Y. H.; Yu, P.; Ramesh, R.; Kalinin, S. V; Pennycook, S. J. Suppression of Octahedral Tilts and Associated Changes in Electronic Properties at Epitaxial Oxide Heterostructure Interfaces. *Phys. Rev. Lett.* **2010**, *105* (8), 87204.

(48) Borisevich, A.; Ovchinnikov, O. S.; Chang, H. J.; Oxley, M. P.; Yu, P.; Seidel, J.; Eliseev, E. A.; Morozovska, A. N.; Ramesh, R.; Pennycook, S. J.; Kalinin, S. V. Mapping Octahedral Tilts and Polarization Across a Domain Wall in $BiFeO_3$ from Z-Contrast Scanning Transmission Electron Microscopy Image Atomic Column Shape Analysis. *ACS Nano* **2010**, *4* (10), 6071–6079.

(49) Levin, I.; Krayzman, V.; Cibin, G.; Tucker, M. G.; Eremenko, M.; Chapman, K.; Paul, R. L. Coupling of Emergent Octahedral Rotations to Polarization in $(K,Na)NbO_3$ Ferroelectrics. *Sci. Rep.* **2017**, *7* (1), 15620.

Table of Contents Graphic

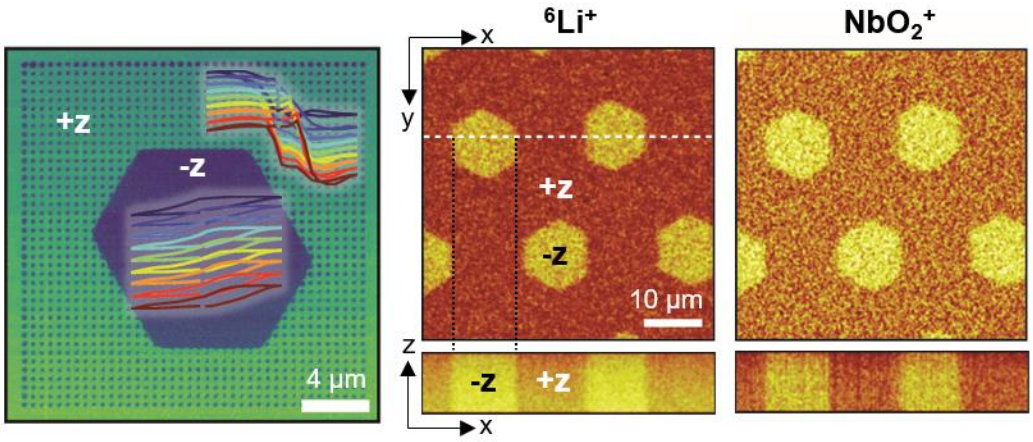
+z
-z
4 μm
x
y
z
x
$^6Li^+$
+z
-z
10 μm
-z
+z
NbO_2^+